Mineralogical analyses and in vitro screening tests for the rapid evaluation of the health hazard of volcanic ash at Rabaul volcano, Papua New Guinea

Mineralogical analyses and *in vitro* screening tests for the rapid evaluation of the health hazard of volcanic ash at Rabaul volcano, Papua New Guinea

Jennifer S Le Blond[1,2*], Claire J Horwell[3], Peter J Baxter[4], Sabina AK Michnowicz[3], Maura Tomatis[5], Bice Fubini[5], Pierre Delmelle[6], Christina Dunster[7], Herman Patia[8],

[1]Department of Geography, University of Cambridge, Downing Place, Cambridge, CB2 3EN, UK.

[2]Department of Mineralogy, Natural History Museum, Cromwell Road, London, SW7 5BD, UK.

[3]Institute of Hazard and Risk Research, Department of Earth Sciences, Durham University, Science Labs, South Road, Durham, DH1 3LE, UK.

[4]Institute of Public Health, University of Cambridge, Cambridge, CB2 2SR, UK.

[5]Dipartimento di Chimica I.F.M., Interdepartmental Center "G. Scansetti" for Studies on Asbestos and other Toxic Particulates, Università degli studi di Torino, Via P. Giuria 7, 10125, Torino, Italy.

[6]Environment Department, University of York, Heslington, York, YO10 5DD, UK.

[7]Lung Biology Group, Pharmaceutical Science Division, King's College London, SE1 9NH, UK.

[8]Rabaul Volcano Observatory, P O Box 386, Rabaul, East New Britain Province, Papua New Guinea.

[*]E-mail: jl490@cam.ac.uk, Telephone: +44 (0)1223 339819, Fax: +44 (0)1223 333392.

Abstract

The continuous ash and gas emissions from the eruptive activity at the Tavurvur in the Rabaul caldera, Papua New Guinea, in 2007-08 impacted on nearby populations and the environment. As part of a formal evaluation of the effects of volcanic emissions on public health, we investigated the potential health hazard of the ash using a suite of selected mineralogical analyses and *in vitro* toxicity screening tests. The trachy-andesitic ash comprised 2.1-6.7 vol. % respirable (sub-4 μm diameter) particles. The crystalline silica content was 1.9–5.0 wt. % cristobalite (in the bulk sample) with trace amounts of quartz and/or tridymite. Scanning electron microscopy showed the ash particles were angular with sparse, fibre-like particles (~3-60 μm max. diameter) observed in some samples, which we confirmed to be $CaSO_4$ (gypsum) and not asbestiform fibres. The ash specific surface area was low (0.1–2.7 m^2g^{-1}). Ash samples generated potentially-harmful hydroxyl radicals through an iron-mediated catalytic reaction, in the range of 0.15-2.47 μmol m^{-2} (after 30 min of reaction). However, *in vitro* study of particle oxidative capacity (potential oxidative stress reaction using artificial lung lining fluid) and quartz-like injury to red cells (erythrolysis assay) nevertheless revealed low biological reactivity. The findings suggest that acute exposure to the ash would have a limited potential to exacerbate pre-existing conditions such as asthma or chronic bronchitis, and chronic exposure was unlikely to lead to silicosis.

Key words: health hazard, Rabaul, risk assessment, volcanic ash, multidisciplinary.

Introduction

Rabaul volcano, Papua New Guinea (PNG), entered a new eruptive phase in 1994 with a Plinian event involving the simultaneous eruption of Tavurvur and Vulcan cones ending a period of repose dating from the 1940s. Since 1994, Tavurvur has shown intermittent eruptive activity. The most recent ash emission crisis began after a sub-Plinian event on 7th October 2006, with increased gas and ash emissions that became continuous during 2007-08. The severe air pollution caused by the particulate matter (PM) and gas raised concerns for the respiratory health of approximately 70,000 people living downwind of the volcano. Exposure to the plume occurred mainly during the dry season when the prevailing winds blow the plume over the area for six months of the year, before reversing their direction in the wet season. We present the results of a rapid mineralogical investigation of the ash (incorporating grain size, bulk composition, particle morphology and composition, and crystalline silica content) to study its potential for causing acute and chronic adverse health effects on the respiratory system, and additional in vitro toxicity screening tests (surface hydroxyl radical generation, particle oxidative capacity and erythrocyte lysis assay) to assess its inflammatory potential in the lung.

Scientific knowledge about the effects of exposure to air pollution has increased exponentially in the last two decades, especially in research relevant to the health effects of airborne PM in urban and non-urban environments (WHO 2006). A limited number of studies have been undertaken during volcanic eruptions, to determine the potential human respiratory health effects of the PM_{10} fraction of ash (PM of aerodynamic diameter sub-10 μm), a key metric in air pollution monitoring (Horwell and Baxter 2006 and references

68 therein). Volcanic emissions containing respirable sized ash particles (sub-4 μm
69 diameter) have been found to provoke acute respiratory symptoms in individuals with
70 chronic lung diseases living in areas impacted by ash fall, for example at Mount St
71 Helens, 1980 (Horwell and Baxter 2006). During long-lived eruptions, exposure to
72 repeatedly-raised concentrations of respirable crystalline silica (RCS) in some types of
73 volcanic ash could potentially cause silicosis (a disabling fibrogenic lung disease), and an
74 associated increase in the risk of lung cancer (Horwell and Baxter 2006; IARC 1997;
75 Yano et al. 1986). The fibrogenic properties of RCS (silicosis) and asbestos or
76 asbestiform fibres (asbestosis) have been well recognised in industrial settings for many
77 years, where mineral dusts are routinely analysed for the presence of RCS or fibres to
78 meet occupational health and safety regulations.
79
80 Volcanic ash emissions can affect populations over wide areas and, once deposited, ash
81 can become re-suspended in the ambient air by human activity or the wind and adversely
82 affect air quality. High exposures to volcanic PM can occur in outdoor workers (for
83 example, those employed in remediation efforts after an ashfall) and often necessitate
84 using respiratory protection, as well as measures to suppress the re-suspension of ash.
85 The first large-scale investigation of the health hazards of volcanic PM began soon after
86 the cataclysmic eruption of Mount St Helens in 1980, which blanketed populated areas in
87 the northwestern USA with ash. Mineralogical studies initially found a wide range of
88 values for the concentration of RCS, with considerable confusion over the appropriate
89 analytical methods to adopt. Similar concerns arose at the on-going eruption of the
90 Soufrière Hills volcano, Montserrat where, unlike at Mount St Helens, the population has

been frequently exposed to abundant sub-10 μm PM containing elevated amounts of cristobalite, a crystalline silica polymorph. Epidemiological surveys, toxicological studies and related ash analysis techniques were slowly developed during these landmark eruptions, as summarised by Horwell and Baxter (2006). Since then, the importance of having a rapid response to meet public health concerns in eruptions has become evident, and this paper defines a selected suite of mineralogical analyses and *in vitro* toxicity screening tests that can be used in a single comprehensive investigation of samples of ash to evaluate their health hazard.

Geological setting

Rabaul caldera (688 m asl) is located on the northeastern tip of New Britain Island (4° 16′ 15.6″ S, 152° 12′ 10.8″ E), PNG (Fig. 1). At least 5-9 caldera forming eruptions have occurred at Rabaul during the last 20 ka (Nairn et al. 1995). The latest of these major eruptions occurred 1400 years ago and breached the southeastern wall to form Blanche Bay, a natural sheltered harbour (Heming 1974). At least 8 intra-caldera eruptions have occurred since the 1400 year BP event building small pyroclastic and lava cones inside the caldera (Nairn et al. 1995). Vulcan and Tavurvur are cones located on opposite sides of the caldera (Fig. 2), that have been the two most active centres over the last 130 years.

Historically, volcanism at Rabaul caldera has been dominated by two main eruption types: a) basaltic and basaltic-andesitic cone building Strombolian eruptions and b) dacitic (and more rarely rhyolitic) Plinian eruptions. There is a record of effusive and

pyroclastic eruptions from Rabaul, dating back to 1767 (McKee et al. 1985). The main eruptive periods in 1878 and 1937-1943 and 1994 involved simultaneous vent eruptions from Tavurvur and Vulcan in the caldera (Nairn et al. 1995).

It is estimated that around 70,000 people reside within a 15 km radius of Rabaul caldera (Smith, 2001). Previous eruptions at Tavurvur have been explosive, or produced lava flows and dome extrusion (Global Volcanism Program). After the devastating eruption in 1994, the provincial capital was moved from Rabaul to Kokopo (Blong and McKee 1995), but the harbour at Rabaul (the third largest in PNG) is vital to the economy of New Britain.

Tephra composition

The ash from both Vulcan and Tavurvur vents appears to be water-modified (i.e. fine grained, poorly vesiculated, angular ash (Nairn et al. 1989)). The similarities in the bulk ash composition from Tavurvur and Vulcan suggest that both vents share the same magma chamber (Johnson et al. 1995; Roggensack et al. 1996). The composition of the ejecta from Vulcan and Tavurvur did not alter significantly over the period 1878 to 1937-1994 and can be classified as generally andesitic to dacitic (~61-63 wt. % SiO_2), although there have been a few basaltic enclaves (Cunningham et al. 2009). It was thought there may have been an increase in magma production (which resulted in a more frequently recharged magma chamber with less-differentiated melts), perhaps due to episodic faulting within the caldera, which caused andesitic, as well as dacitic, magma production (Wood et al. 1995). Some information is available on the composition of ash from

Tavurvur since 1994 (Cioni and Rosi, personal communication): Cioni and Rosi sampled the sequences of ejecta material from Tavurvur and Vulcan in February 2002 and found no clear compositional changes with time, suggesting that the magma had not changed substantially from the andesitic-dacitic ejecta sampled before 1994.

Methods

We obtained samples of ash emitted from the Tavurvur and Vulcan vents from the 1994 eruptions, and samples from the subsequent eruptions at Tavurvur until April 2008. Table 1 summarises the details of the ash samples and analysis techniques used. Sample Tav R2 was tested with all techniques as it represents a recent, well-sourced sample. For comparison, ash samples from Langila and Manam (Fig. 1) volcanoes (also in PNG) were included in this study.

Sample preparation

Prior to analysis, all samples were dried in an oven (<90 ^{o}C) for 24 hours and sieved through 1 mm and 2 mm sieves to maintain the 'ash fraction' (<2 mm) and to remove large particles which could damage the particle size analyser.

Morphological and compositional analyses

Bulk composition

Ash samples were analysed on the PANalytical Axios Advanced X-ray fluorescence (XRF) spectrometer at the Department of Geology, University of Leicester, UK. Major elements were determined on fused glass beads prepared from ignited powders, with a

160 sample to flux ratio 1:10, 100 % Li tetraborate flux. Bulk oxide elemental composition
161 was determined which allowed us to identify the magma type presently being erupted
162 from the volcanic vents at Rabaul caldera.
163
164 *Particle size*
165 The grain-size distribution (from 0.2 μm to 2000 μm) was determined using a Malvern
166 Mastersizer 2000 laser diffractometer with a Hydro MU attachment and ultrasonics, at the
167 Department of Geography, University of Cambridge, UK. Water was used as a
168 dispersant, with a pump speed of 2500 rpm, obscuration of 5-20 % and a measurement
169 time of 10 sec. The refractive index was set at 1.63 (for the andesitic samples) and 1.55
170 (for Manam and Langila, basaltic samples) and the absorption coefficient of 0.1, based on
171 the findings reported in Horwell (2007). The average of three readings was taken for each
172 sample, given as volume percent that was then converted into cumulative volume percent
173 to determine the quantity of material in the relevant size fractions for assessing health
174 risk. The weight data from any sieved particles in the 1-2 mm size range (still within the
175 accepted 'ash fraction') was recorded and then re-incorporated into the grain size
176 distribution calculations after the analysis.
177
178 *Crystalline silica content*
179 X-ray diffraction (XRD) enables identification of the crystalline components in a bulk-
180 powdered sample. A new, rapid quantification technique known as the Internal
181 Attenuation Standard (IAS) method (Le Blond et al. 2009) has been used here to quantify
182 the weight percentage of cristobalite and quartz in the bulk Rabaul ash samples.

183 Crystalline silica polymorphs have been singled out for quantification because they
184 cause the fibrotic lung disease silicosis and are classed as human lung carcinogens (IARC
185 1997).
186
187 The bulk ash samples were ground with an agate pestle and mortar, to reduce the grain
188 size to (approximately) between ~5-20 μm diameter. Initially, a small sub-sample was
189 smeared onto a quartz substrate and analyzed for the identification of the crystalline
190 phases. An Al deep well mount was created for the quantitative (IAS) experiments. XRD
191 data were collected using an Enraf-Nonius X-ray diffractometer with an INEL curved
192 position sensitive detector (PSD) at the NHM, UK (for details on sample preparation and
193 instrument setup see Le Blond et al. 2009).
194
195 *Particle morphology*
196 Scanning electron microscopy (SEM) was used to investigate particle morphology.
197 Analysis was carried out using the Philips XL-30 field emission SEM (at the Natural
198 History Museum (NHM), London, UK), which has a maximum resolution down to 2 nm.
199 Al stubs were polished and thoroughly cleaned. Ethanol was applied to the surface of the
200 stub to enable the sprinkled ash particles to adhere onto the surface. After a drying period,
201 the stub was coated with 25 nm of gold.
202
203 *Particle composition*
204 Whilst experimental data on atmospheric particles indicate that particle size and
205 correlated parameters, number and surface area, are important metrics in eliciting health

206 effects, chemical composition is believed to be central to understanding of particle
207 toxicity (e.g. Harrison and Yin 2000). A LEO 1455VP SEM with Oxford INCA energy
208 dispersive X-ray analysis system (EDX) (at the NHM, UK) was used to determine the
209 elemental composition of individual particles in the sample. For SEM-EDX analysis, ash
210 was sprinkled onto Al stubs with carbon sticky tabs and carbon coated (~25 nm). SEM-
211 Raman was also carried out on some of the ash samples, at Renishaw Plc,
212 Gloucestershire, UK. SEM-Raman is used to accurately identify the mineralogical
213 composition of individual particles. Unlike SEM-EDX, SEM-Raman can distinguish
214 between the different polymorphs of the same mineral (e.g. the silica polymorphs –
215 quartz, cristobalite and tridymite). For SEM-Raman, particles were sprinkled on plain Al
216 stubs and left uncoated (as carbon is an efficient Raman scatterer and would interfere
217 with mineral identification).
218
219 Interaction between the volatile components and the ash particles in the volcanic plume
220 may lead to the deposition of more or less soluble compounds onto the ash surfaces (e.g.
221 Witham et al. 2005). As a result, an array of elements, including known toxic metals such
222 as Pb, As, Cd, Ni, Cr, Mn, V and Hg, can be released from the ash surface upon contact
223 with water and, by analogy, with fluids found in the lung. Soluble Fe is also of interest,
224 since Fe contributes to particle-induced formation of reactive oxygen species through the
225 Fenton reaction (e.g. Kelly 2003; Fubini et al. 1995). Leachate analysis was carried out as
226 part of the suite of analyses undertaken to determine both the health and environmental
227 impact of the ash from Rabaul. A 1 g sub-sample of Tav R2 was shaken with 25 ml of
228 neutral-pH deionised water for 1.5 hrs, then the extract was filtered on a 0.45 μm pore

229 filter paper (Witham et al. 2005). Fe, As, Cd, Co, Cr, Cu. Mn, Ni, Pb and Zn in the water
230 extract were measured by inductively coupled plasma – optical emission spectroscopy
231 (ICP-OES) and fluoride by ion chromatography (IC) both at the University of York.
232
233 Analyses testing for potential toxicity
234 *Particle specific surface area and reactivity*
235 The specific surface area and the surface reactivity of selected fine-grained samples were
236 measured as proxies for particle toxicity potential within the lung. A Micromeritics
237 TriStar 3000 Surface Area and Porosimetry Analyser in the Department of Chemistry,
238 Durham University, UK was used to determine the surface area. This equipment employs
239 the BET (Brunauer Emmet Teller) method of specific surface area analysis using
240 nitrogen. Prior to analysis, all the samples were degassed (under N_2) at 150 ^{o}C for at least
241 2 hrs (e.g. Gregg and Sing 1982).
242
243 Particle surface reactivity can be determined by the particles' ability to generate free or
244 surface radicals (Fubini and Hubbard 2003; Fubini and Otero Arean 1999; Hardy and
245 Aust 1995; Ghio et al. 1992). Fe-catalyzed free radical production is known to potentially
246 be a contributor to both lung inflammation and carcinoma (Hardy and Aust 1995; Kane
247 1996). Recent work by Horwell et al. (2007; 2003a) has shown that certain volcanic ash
248 samples generate abundant hydroxyl radicals in the presence of hydrogen peroxide (found
249 naturally in the lung) via the Fenton reaction. Hydroxyl radical production is particularly
250 pronounced in basaltic ash samples (Fe-rich), which have been previously considered to

have a low respiratory health hazard due to their low crystalline silica content (Horwell et al. 2007).

Electron Paramagnetic Resonance (EPR) spectroscopy in association with the spin-trapping technique is employed to quantify the free radicals generated by volcanic ash (Shi et al. 1995; Fubini et al. 1995; 2001; Horwell et al. 2003a; 2007). The method replicates the Fenton reaction that may occur in the lung. To simulate this reaction 150 mg of the ash sample is suspended in 500 μL 0.5 M phosphate buffered solution at pH 7.4 (the pH of lung fluids), then 250 μL of 0.15 DMPO (the spin trap; 5,5'-dimethyl-1-pyrroline-*N*-oxide) and 500 μL H_2O_2 (0.08 M) are added and the suspension stirred for 1 hour. Aliquots of the suspension are withdrawn from a darkened vial after 10, 30 and 60 min and filtered through cellulose acetate (0.25 μm porosity) filters. The liquid is introduced into a 50 μL capillary tube and placed in a Miniscope 100 ESR spectrometer (Mag-nettech at the Università degli Studi di Torino, Italy). The following parameters were used: receiver gain 9×10^2, microwave power: 10 mW, modulation amplitude: 1 G, scan time: 80 sec, number of scans: 2. Each sample was tested at least twice and an average taken. The integrated amplitude of the peaks generated in each spectrum is proportional to the amount of radicals generated. The number of radicals is calculated by including a solid solution of Mn^{2+} in $CaCO_3$ as a calibration standard. Since samples exhibit differences in surface area, results are expressed on a per unit surface area basis (i.e. combined with the BET results) to reveal the true reactivity of the surface.

The amount of removable ferrous (Fe^{2+}) and ferric (Fe^{3+}) Fe on the ash particle surface, which represents the Fe available for the Fenton reaction, was also measured. Removable Fe^{2+} was measured through the use of ferrozine, a bidentate N donor chelator (pH 4) specific for Fe^{2+}, following a method previously described (Hardy and Aust 1995; Horwell et al. 2003a; 2007). Ascorbic acid reduces the Fe^{3+} (to Fe^{2+}) and is used in half of the experiments to measure the total amount of Fe mobilized. Ash samples (20 mg) were placed in tubes with 20 mL of 1 mM solutions of just ferrozine or ferrozine and ascorbic acid (1 mM). The suspensions were stirred at 37 °C. After 24 hours the samples were removed, centrifuged for 15 min and an aliquot of the supernatant was analysed in a Uvikon 930 dual beam spectrophotometer (Kontron Instrument) (562 nm, E_{mM} = 27.9 mM^{-1} cm^{-1}) at the Università degli Studi di Torino, Italy. The samples were then returned to the incubator and measured in this way every 24 hours for 9 days. The ferrozine forms a coloured complex with Fe^{2+}. A control solution of ferrozine with water showed no colour change over the experiment. As with the EPR experiments, the available Fe results are combined with the BET results and expressed per unit surface area.

Particle oxidative capacity

Particle oxidative capacity is a measure of the potential oxidative stress induced by a sample of PM within the lung. The respiratory tract lining fluid is the first physical defence encountered by inhaled particles entering into the respiratory system and is known to contain antioxidants such as ascorbate (Willis and Kratzing 1974; Skoza et al. 1983; van der Vleit et al. 1999). In healthy individuals, most of the endogenous antioxidants are induced in response to slight changes in cellular redox status as a result

296 of particle interaction within the lung. Cellular redox state can be altered by the
297 introduction of oxidising species (such as redox active transition metals (Mudway et al.
298 2004)) absorbed on the particle surface. The potential for inhaled particles to provoke
299 oxidative injury within the lung is, therefore, predominantly controlled by the reaction of
300 the antioxidant defences (pro-oxidant and pro-inflammatory responses) (Ayres et al.
301 2008). The strength of an individual's antioxidant defence is also an important
302 consideration, as asthma sufferers can have an enhanced sensitivity to air pollutants, due
303 to their impaired antioxidant defences (Kelly et al. 1999; Li et al. 2003)
304
305 The oxidative potential of ash particles can be quantified, and the reactions likely to occur
306 *in vivo* at the air-lung interface inferred, by monitoring the depletion of the antioxidant
307 during the incubation of ash with ascorbate over time (at 37 ^{o}C, pH 7.4) (Ayres et al.
308 2008). The oxidative capacity of the ash was measured, at King's College, London, in
309 order to elucidate a more complete understanding of *in vitro* toxicity. A known weight of
310 Tav R2 was re-suspended in 5 % methanol/95 % chelex-treated water at pH 7.0 at 150 μg
311 ml^{-1}, sonicated and an aliquot diluted to 12.5 μg ml^{-1}. Triplicate aliquots were incubated
312 for 10 min at 37 ^{o}C in 96 multiwell plate, followed by the addition of a final
313 concentration of 200 μM ascorbate solution. In house controls (negative control carbon
314 black and positive control ROFA) were run simultaneously. All samples were run at a
315 final concentration of 10 μg ml^{-1}. A Spectramax 190 platereader (Molecular Devices) set
316 to 265 nm, 37 ^{o}C with associated SoftMaxPro software was used to record the decrease in
317 ascorbic acid absorbance every 2 min and monitored for a total of 2 hours.
318

Erythrocyte Lysis Assay (haemolysis)

Red blood cells (erythrocytes) transport oxygen in the blood and are at risk of oxidation injury from endogenous substances (e.g. hydrogen peroxide is often produced in response to inflammation), or exogenous chemicals. The erythrocyte lysis assay has been used for over two decades to screen mineral dusts for bio-reactivity. Erythrocytes were obtained from fresh human venous blood and the washed erythrocytes were incubated with NaCl (negative control), TiO_2 (rutile and anatase polymorphs), DQ12 quartz (known to cause red blood cell haemolysis), an ash sample (Tav R2) and Triton x (positive control) (Sigma) for a period of 20 min. The subsequent % haemolysis was determined by measuring the absorbance at 550 nm. All particles were probe sonicated for 5 min prior to use in the assay. Haemolysis analysis was carried out at the Centre for Inflammation Research, University of Edinburgh, UK.

Results

Bulk composition

The samples were found to range from basaltic, basaltic-andesite to trachy-andesite (i.e. mafic to intermediate) (Fig. 3). The Tavurvur samples are all trachy-andesitic with the exception of Tav 00 which appears more mafic than the other Rabaul volcano samples. XRF data show that this sample has elevated Ca and S and a high loss on ignition (LOI) value.

Particle size

341 The data from the Malvern Mastersizer 2000 are presented according to the health-
342 pertinent size fractions (from Horwell 2007). In general, the Tavurvur samples are fairly
343 similar in size distribution (Table 2). The proportion of particles sub-4 μm in diameter
344 varies from 4.5-6.5 vol. %. This variation may be due to a number of factors including
345 eruptive behaviour (explosivity, plume dynamics, magma composition) but also the
346 location of collection of samples with respect to the volcano.
347
348 The samples from Manam and Langila are generally coarser than the Tavurvur samples
349 and have 3.3 and 3.5 vol. % sub-4 μm, respectively. These samples are also more basaltic
350 than the Tavurvur/Vulcan samples (Fig. 3) and their coarseness probably reflects a more
351 effusive eruption style. The Tav R2, R3, R4 and R6 are almost identical in terms of
352 quantity of respirable particulate although the Tav R2 and R3 samples have a higher
353 proportion of material sub-63 μm in diameter, compared with R4 and R6.
354
355 Most of the Tavurvur samples have a similar grain size distribution to samples measured
356 from the 1997 explosive eruptions of the Soufrière Hills, Montserrat (andesitic magma,
357 Vulcanian explosion) or the eruption at Tungurahua, Ecuador (andesitic magma,
358 Strombolian-Vulcanian) (Horwell 2007), which is in keeping both with their andesitic
359 composition (Fig. 3) and with the mildly-explosive nature of the eruptions (VEI 2-3). The
360 more basaltic samples from Manam and Langila are similar in vol. % distribution to that
361 found for other basaltic eruptions such as the 1976 eruption of Fuego, Guatemala
362 (basaltic magma, sub-Plinian) or from Mt. Etna, Italy (basaltic, Strombolian) although
363 these eruptions were unusually explosive (VEI 3-4) (Horwell 2007).

364

365 Crystalline silica content

366 Table 3 gives the quantification results for the crystalline silica polymorph cristobalite.
367 Both tridymite (which had an identifiable peak, just above background level) and quartz
368 were too scarce to be quantified. The samples from 2005 onwards are relatively similar
369 and have cristobalite values between 2-3 wt. %. The greatest cristobalite concentrations
370 are seen in the 1998 samples (4.6–5.0 wt %).

371

372 Until recently quantitative determination of mineral phases in a heterogeneously
373 composed dust has been problematic, particularly if the mineral assemblage is not known
374 in advance. The new Internal Attenuation Standard (IAS) method (see Le Blond et al.
375 2009 for details) of crystalline silica quantification within samples of volcanic ash has
376 been tested successfully on samples of ash from the Soufrière Hills volcano, Montserrat
377 and Chaitén volcano, Chile (Horwell et al. in press), and Vesuvius, Italy (Horwell et al.
378 submitted). The ash from these volcanoes have cristobalite contents that range from <2 to
379 ~18 wt. % in the bulk ash samples. It should be noted that results presented here, and in
380 the Horwell et al. papers, are for the wt. % of crystalline silica polymorphs in the bulk ash
381 sample and not the sub-4 or sub-10 μm PM fractions in which the crystalline silica
382 minerals may be further concentrated (Horwell et al. 2003b).

383

384 Particle morphology

385 The general morphology of the ash is similar to many other volcanic ash samples (e.g.
386 Horwell and Baxter 2006; Horwell et al. 2003b), but in several samples, including those

387 from Manam and Langila, we found micron-sized, fibre-like particles (Figs. 4 and 5). We
388 know of only three previous investigations that have identified fibrous-looking material
389 in freshly erupted volcanic ash (1) nano-sized cristobalite fibres from Chaitén, Chile in
390 May 2008 (Reich et al. 2009); 2) plagioclase/glass micro-fibres also from Chaitén, Chile
391 (Horwell et al. in press), 3) gypsum micro-fibres in ash erupted from Halema`uma`u
392 Crater, Kilauea Volcano, Hawai'i (March-April 2008) (Horwell et al. 2008), although
393 they have been observed previously in airborne particulate samples generated as basaltic
394 lava enters sea water at Kilauea, Hawai'i (Kullman 1994) and in core samples extracted
395 from the hydrothermally-altered lavas beneath Kilauea (Bargar et al. 1995). SEM images
396 (Figs. 4 and 5) show ash-sized blocky particles, fibre-like particles and numerous
397 particles sub-4 μm (i.e. respirable). The largest fibre-like particle imaged was ~60 μm
398 along the longest axis (in Lang 07) and the smallest was approximately 4 μm in length.
399 The short axis was usually between <1 μm and 3 μm diameter. The aspect ratio of these
400 fibre-like particles conforms to the WHO definition for fibres (WHO 1986) which is used
401 by regulatory authorities in their classification and measurement of asbestos fibres, but
402 we established that these needle-shaped particles cannot be described as asbestiform: a
403 term which is used to describe minerals in which fibres have a high tensile strength and
404 flexibility and are insoluble in the lung. Here we found that the fibre-like particles were
405 easily broken with light milling and were too short to display flexible morphology. They
406 also did not display the 'fibril' morphology typical of tremolite (see Skinner et al. 1988).
407
408 The samples did vary in the number of fibre-like particles that could be found and
409 analysed under the SEM. In general, it was much easier to locate the fibre-like particles in

410 the more recent samples, for example Tav R2 and R3 and Lang 07. Samples R4 and R6
411 had fewer fibre-like particles than R2 and R3 samples. Overall, however, the fibre-like
412 particles were sparse.
413
414 Particle composition
415 The MDHS (1998) Guidance on the discrimination between fibre types in samples of
416 airborne dust on filters during SEM advises that, "*Gypsum and anhydrite needles can*
417 *resemble amphibole asbestos morphologically; they are distinguished easily by their*
418 *EDXA* [EDX] *spectra which contain calcium and sulphur (sometimes with a little*
419 *aluminium) in contrast to elements in the amphiboles"*. This was the case in this study.
420 When the fibre-like particles were probed by SEM-EDX, the X-ray spectra, in most
421 cases, had two peaks (Ca and S) (Fig. 6(b) and (c)), roughly of equal size (reflecting the
422 atomic formula $CaSO_4(.H_2O)$ for gypsum/anhydrite). Mineralogical analysis by SEM-
423 Raman further confirmed that the Ca-S fibre-like particles were either gypsum
424 ($CaSO_4.2H_2O$), anhydrite ($CaSO_4$) or hemi-hydrite (a hybrid form of gypsum and
425 anhydrite). We were unable to identify the exact composition for some fibre-like
426 particles; often the fibre-like particle would have a gypsum spectrum except it would be
427 lacking the OH spectral peaks at ~3500 cm^{-1} (Fig. 8). This may be indicative of hemi-
428 hydrite. The Tav 00 sample contained ash-sized blocks of anhydrite. Here, SEM-Raman
429 spectra were clearly identifiable as anhydrite and it may be that the Raman spectrometer
430 was unable to obtain such clear spectra for the much smaller fibre-like particles.
431 Alternatively, the fibre-like particles are likely to have formed very rapidly and may not
432 sustain the exact crystalline morphology of a well-formed crystal, hence giving less

433 defined Raman spectra. Not all of the samples from the Rabaul sample suite were
434 analysed as previous SEM investigation had revealed that only the R2, R3 and Lang 07
435 samples had sufficiently numerous fibre-like particles to warrant compositional analysis.
436
437 Elemental mapping was carried out on a fibre in the Tav R2 sample. The Si seen in Fig.
438 7(d) is markedly reduced in comparison to the surrounding silicate particles and we
439 attribute the presence of Si to smaller particles adhering to the fibre-like particle, as can
440 be seen in the backscatter image (Fig. 7(a)).
441
442 Leachate analysis
443 The ash leachate analysis (Table 3) gives concentrations of As, Mn, Co, Ni, Cu, Zn and
444 Cd ranging from 0.023 to 10.25 mg kg^{-1}. Fe was below the detection limit (~0.1 mg kg^{-1}).
445 The ash leachate was slightly acidic with a pH of 5.6.
446
447 Particle specific surface area and reactivity
448 The specific surface area measured ranged from 0.2 $m^2 g^{-1}$ (Tav 05) to 2.7 $m^2 g^{-1}$ (Vul
449 94N) (Table 4). The upper limit of the range is slightly higher than previously published
450 specific surface area data for bulk ash (0.2-1.8 $m^2 g^{-1}$, n = 12) (Horwell et al. 2007), but is
451 still low when compared to other toxic powders, e.g. Min-U-Sil 5 quartz standard (U.S.
452 Silica, Berkeley Spring plant) which has a surface area of 5.2 $m^2 g^{-1}$.
453
454 Fig. 9 shows the hydroxyl radical generation results over the 60 min of each experiment.
455 All samples generated the hydroxyl radical and showed similar reactivity over the

456 duration of the experiment. The only exceptions are the samples from Vulcan and TAV
457 00, which generated few hydroxyl radicals. There were no consistent differences in the
458 kinetics, except for Tav R4 that showed a linear increase of radical yield.
459
460 The results of the iron release experiments, are shown in Fig. 10 and expressed per unit
461 surface area during 9 days of incubation both for removable Fe^{2+} (Fig. 10a - ferrozine
462 solution) and for total removable Fe (Fig. 10b - ferrozine solution containing also
463 ascorbic acid as a reducing agent). Comparable amounts of Fe ions in both oxidation
464 states were extracted from the surface of the ash samples. As expected from the silicic
465 composition of the samples (Fig. 4), all of the Tavurvur samples displayed relatively low
466 Fe release in comparison to the basaltic Manam sample. The only exception is Langila
467 which, along with Manam, had raised Fe_2O_3 content (from XRF analysis, Table 5) as
468 would be expected for a more mafic sample, but the Langila sample does not seem to
469 have a commensurate amount of available Fe for reaction.
470
471 The correlation between the amount of hydroxyl radicals generated after 30 min of
472 incubation and the amount of Fe released (in both oxidative states) after 7 days of
473 incubation is shown in Fig. 11(a). Some samples of ash with little removable Fe are
474 capable of generating plentiful radicals. With respect to previously published results, Fig.
475 11(b) compares the PNG samples with four samples of volcanic ash previously analysed
476 by Horwell et al. (2007). Here, these samples were re-analysed, and both new and old
477 data compared well. Fig. 11(b) shows that the Etna ash (basaltic) is capable of generating
478 more radicals, and has more available Fe, than any of the PNG samples. Another basaltic

479 sample (Cerro Negro) is very similar to the basaltic Manam sample. The Tavurvur
480 trachy-andesitic samples all compare well with the andesitic Soufrière Hills, Montserrat
481 and Pinatubo samples. The capacity of samples of similar Fe availability to generate a
482 range of radical quantities is explained by Horwell et al. (2007) as being due to the fact
483 that an excess of Fe in certain co-ordination states at the surface can, in fact, reduce the
484 reactivity of a particle (Fubini et al. 2001), suggesting that the ability to generate radicals
485 depends on the presence of isolated Fe ions adhered to the surface.
486
487 Particle oxidative capacity
488 The oxidation kinetics of re-suspended samples was calculated as nmol l^{-1} of ascorbate
489 oxidised sec^{-1} (Fig. 12). A 1-way ANOVA (Tukey) test was performed on the data to
490 determine whether there was any significance observed ($p<0.05$). No significant increase
491 in ascorbate oxidation was observed when the Tav R2 sample was present in the
492 incubation. Both positive and negative controls displayed the expected outcomes during
493 the experiment and a comparison can be seen for particles collected on London roadsides
494 (Urban PM10a and b).
495
496 Erythrocyte Lysis Assay (haemolysis)
497 Results are presented here both as % haemolysis per unit mass (Table 6) and per unit
498 surface area (Fig. 13). Once surface area is taken into account it can be seen that, per unit
499 surface area, volcanic ash induced significantly more haemolysis than the low-toxicity
500 TiO_2 polymorphs (rutile and anatase) but is still much less toxic to red blood cells than
501 the DQ12 quartz standard. Although the surface area normalised results are revealing

about the relative harmfulness, exposure measurements to meet health and safety legislation are based on the mass metric and, on this basis, the ash is much less harmful than quartz. It should be recognised, however, that volcanic ash is a mixed dust containing diluted concentrations of potentially-toxic minerals, so its toxicity is unlikely to match a pure standard.

Discussion

The Rabaul ash contains fairly low amounts of sub-10 μm PM, in comparison to ash from other andesitic volcanoes (Horwell 2007), in keeping with the mild explosive nature of the eruptions. The amount of respirable, sub-4 μm material is also low, typically just less than half of the sub-10 μm PM fraction (Horwell 2007), but the *number* of small particles in this fraction will be very high. On a by-weight or by-count basis the hazard will ultimately depend upon the actual individual's exposure.

The next most important consideration is the RCS content (1-5 wt % measured in bulk samples). The presence of cristobalite in the Rabaul ash may be related to crystallisation from hydrothermal fluids and the incorporation of hydrothermally-altered rock. The lack of quartz is expected from descriptions of the petrology of the andesitic products at Rabaul (Wood et al. 1995). Although the RCS content is low in comparison with exposure in occupational studies of workers who develop silicosis, it is nevertheless of concern when the exposure is continuing for up to 24 hours a day in a population that also contains sick adults and children who may be more susceptible to the dust than healthy adults. One other important consideration is the adverse impact that prolonged exposure

525 to high levels of ash containing RCS might have on this population with its high
526 prevalence of tuberculosis. RCS is known to increase the risk of developing tuberculosis
527 in occupationally exposed groups in mining and to exacerbate its clinical course (Hnizdo
528 and Murray 1998; teWaterNaude et al. 2006).
529
530 The low bio-reactivity of the ash in the erythrocyte lysis test, however, suggests that the
531 cristobalite is in any case going to be less reactive in the presence of other minerals in the
532 ash, as found in previous studies. Vallyathan et al. (1984) observed a low haemolytic
533 reaction from Mt St Helens ash, and Cullen et al (2002) found a similar result with ash
534 from the Soufrière Hills volcano, Montserrat. In the latter, the cristobalite concentration
535 was much higher than that found here (15-24 wt. % of the sub-10 μm fraction (Baxter et
536 al. 1999)) and would normally present a significant potential to cause fibrotic disease in
537 the absence of other minerals or metals that may markedly reduce its bio-reactivity.
538
539 The oxidative capacity assay found that the Tavurvur ash did not oxidise ascorbate, an
540 assay that simulates the effects of PM on the lining fluid of the lung and the potential of
541 PM to trigger acute symptoms, such as asthma. The apparent differences in results among
542 the hydroxyl radical, oxidative capacity and haemolysis experiments reflect the different
543 mechanisms of toxicity in the lung that the tests are replicating, as they follow different
544 oxidative pathways and involve different cell processes. Therefore, a negative result in
545 one test does not preclude the possibility of toxicity via a different mechanism.
546

547 An unknown factor, which could affect the bio-reactivity results in the older samples (all
548 but R2-R6), was their state of weathering prior to collection. We were not able to obtain
549 detailed information on the origin of these samples, but if the samples were collected
550 from exposed sections in the field, years after eruption (rather than collected fresh at the
551 time of eruption), we might expect that these samples would have been weathered,
552 inducing oxidation and removal of Fe and production of weathered surfaces which reduce
553 hydroxyl radical generation capacity. For example, Horwell et al. (2003a) studied a
554 sample of 'mixed' ash from a section deposited between 1995-2000 at the Soufrière Hills
555 volcano, Montserrat. This aged sample displayed substantially reduced hydroxyl radical
556 generation capacity in comparison to fresh samples analysed. There was, however, no
557 major difference between the surface reactivity results for the Rabaul R-type samples,
558 known to be fresh, and the rest of the sample suite.
559
560 The fibre-like particles observed in the Tavurvur samples raised our immediate concern
561 that they could resemble asbestos minerals. Although many of the observed fibre-like
562 particles found in the Rabaul ash samples conform to the standard definition of a fibre for
563 regulating human exposure (i.e. ≥5 μm in length and have an aspect ratio of 3:1),
564 compositional analysis of the micron-sized fibre-like particles showed that they were
565 almost pure gypsum/anhydrite/hemi-hydrite and not a variety of asbestos (fibrous
566 silicates). Gypsum needles are unlikely to be pathogenic in the lungs with their short half-
567 life (estimated at minutes) as a result of their high solubility (Hoskins 2001; US
568 Department of Heath and Human Service 2006). Epidemiological studies of workers
569 exposed to pure-phase gypsum dust have not found evidence of lung fibrosis or

570 pneumoconiosis (e.g. Burilkov and Michailova-Dotschewa 1990; Einbrodt, 1988; Oakes
571 et al. 1982). In tests on rat and guinea pig lungs, aerosols of calcium sulphate fibres were
572 quickly cleared via dissolution and mechanisms of particle clearance (Clouter et al. 1997;
573 1996). In a chronic inhalation study, Schepers et al. (1955) found that calcined gypsum
574 dust produced minor effects in the lungs of guinea pigs. The fibre-like particles identified
575 in the Rabaul ash therefore can be assumed to be relatively harmless. Further testing to
576 ensure their solubility would include incubating samples in water, hydrochloric acid and
577 simulated lung fluid solutions at different pH levels, to replicate conditions within the
578 lung and within macrophage cells.
579
580 $CaSO_4$ is commonly found in acidic volcanic environments and is formed as a secondary
581 mineral phase by the leaching of the volcanic rock and is often precipitated around
582 volcanic fumaroles (Africano and Bernard 2000). Ohba and Nakagawa (2003) state that
583 gypsum, and other hydrothermal alteration minerals, may be incorporated into volcanic
584 products through; 1) mechanical stripping from hydrothermally altered country rocks by
585 ascending magma, steam or water, 2) sea water-magma interactions, 3) mechanical
586 incorporation from aquifers or surface water into plume, 4) direct precipitation from
587 volcanic fluids. Risacher et al. (2001) also recognised high $CaSO_4$ in the leachate analysis
588 of the ash from eruptions at Lascar volcano, Chile and attributed this finding to the
589 entrainment of ancient sedimentary evaporite-type deposits during the eruption.
590
591 The presence of substantial quantities of blocky anhydrite in the Tav 00 sample explains
592 the XRF data for this sample (Fig. 3). The sample appeared more mafic than the other

593 Rabaul caldera samples. If the anhydrite were removed from the sample, we would
594 expect the sample's composition to be in keeping with the other Rabaul samples.
595
596 The ash from Rabaul readily leached F, Cu, Zn, Mn, As, Ni and Cd upon mixing with
597 water and their concentrations were not exceptional compared to ash from other
598 volcanoes (Witham et al. 2005 and references within). The concentrations of toxic metals
599 in ash leachates are not often measured and vary for different volcanoes and eruptions
600 (e.g. Armienta et al. 1998; Cronin et al. 1997; Cronin and Sharp 2002; Fruchter et al.
601 1980; Hinkley and Smith 1982; Smith et al. 1982; Varekamp et al. 1984). It has been
602 suggested that transition metals, including Fe, Cu and Ni, in respirable aerosols play a
603 role in the inflammatory response of the lung tissues (e.g. Rice et al. 2001), but
604 epidemiological studies have not found any evidence of an association with adverse
605 health outcomes that are substantially greater than for PM (Heal et al. 2009). The
606 oxidative potential of the respirable ash fraction may also be enhanced by the presence of
607 these metals in water-soluble forms, but we found that the Rabaul ash had a low oxidative
608 capacity. Both As and Cd absorbed by inhalation are classified as human carcinogens
609 (IARC 1980; 1993), thus possibly contributing to the health hazard posed by volcanic
610 ash. The slightly acidic pH of the ash leachate is due to the presence of H_2SO_4 and HCl
611 adsorbed onto the ash surfaces (e.g. Hinkey and Smith 1982), which could add to the
612 irritant effect of fine ash on the airways in provoking acute respiratory symptoms.
613
614 Future hazard

615 Over geological history, Rabaul caldera has erupted magma of compositions ranging
616 from basaltic to rhyolitic but the samples analysed for this study all display similar
617 trachy-andesitic compositions. The samples from Manam and Langila volcanoes were
618 more mafic. A change in the style of the eruption at Rabaul should lead to the ash being
619 re-sampled and re-evaluated in case its characteristics as described here will have altered.
620 Future eruptions from Rabaul could switch to basaltic or rhyolitic magma compositions
621 due to large-scale injection of basic magma, magma mixing and fractional crystallisation.
622
623 Rhyolitic eruptions at Rabaul are rare and an eruption of this type would likely be on a
624 much larger, and more explosive, scale than recent eruptions (1994–present day). During
625 such an eruption, we might expect the generation of more fine-grained ash due to the
626 explosivity of the eruption. We would also expect quartz phenocrysts to be present
627 (Wood et al. 1995). We would not necessarily expect to see more cristobalite or gypsum
628 fibres. It is also likely that surface reactivity (i.e. hydroxyl radical generation) would not
629 increase and might even decrease due to the reduction in iron from rhyolitic magmas. The
630 generation of ash might be far greater than recent eruptions, which would force the
631 evacuation of local towns.
632
633 If basaltic eruptions resume, hydroxyl radical generation would be expected to increase,
634 as with the basaltic Manam sample observed here. However, the volume of ash generated
635 would be much lower, and the grain size most probably coarser, compared with the
636 current production (due to effusive emission of lava flows) so local population exposure
637 would be reduced in comparison to current eruptions. It should be noted, however, that

638 basaltic eruptions can be explosive as well as effusive, producing significant quantities of
639 respirable (sub-4 μm) material (e.g. Fuego, Guatemala, 1974) (Horwell 2007). The
640 crystalline silica content would be expected to decrease slightly, but not significantly,
641 given the lack of a mechanism for large-scale cristobalite production.
642
643 **Conclusions**
644 This study is one of the first to apply a selective suite of mineralogical analyses and
645 toxicological screening tests in a single formal evaluation of the health hazards of ash
646 early on in an eruption crisis. The results from our investigation at Rabaul are reassuring
647 in that they suggest that the ash has limited potential to cause acute inflammatory
648 responses leading to attacks of asthma in asthma sufferers and exacerbation of respiratory
649 symptoms in those people with pre-existing respiratory illnesses, such as chronic
650 bronchitis and emphysema. The ash, with its modest RCS content, also appears to have
651 low potential to cause chronic inflammation leading to silicosis. Of concern, however, is
652 the high prevalence of tuberculosis in the local population living in the ash fall area and
653 the lack of availability of, or non-compliance with, anti-tuberculosis medication. Elevated
654 levels of respirable ash in the ambient air for prolonged periods might exacerbate or
655 contribute to respiratory conditions such as tuberculosis, chronic bronchitis and childhood
656 pneumonia. The presence of asbestiform minerals was excluded.
657
658 This study has shown the feasibility of conducting a routine suite of analyses and assays
659 for the preliminary assessment of the health hazard of volcanic ash in a timely manner
660 during an ash emission crisis. The methodologies can be standardised for use in a wide

661 range of volcanic eruptions in the future and provide rapid feed-back for allaying public
662 concerns and for advising health professionals. Clinical and epidemiological studies and
663 routine air monitoring of ash concentration levels in the ambient air are, however, needed
664 to clarify the impact and risk to the population of the health hazards raised in this
665 laboratory investigation.

Acknowledgements

JSL's work is funded by a NERC studentship (Grant No. NER/S/A/2006/14107). CJH acknowledges a NERC Postdoctoral Research Fellowship (Grant No. NE/C518081/2). PJB was funded by the World Health Organization. Thanks to: William Rose (Michigan Technological University, US) for kindly providing the Lang (L5) sample. Nick Marsh at Leicester University for XRF analyses. Gordon Cressey and Hazel Hunter, NHM, London for XRD advice and support. Neil Cameron et al. Durham University, for BET analyses advice. Raffaello Cioni (Universita degli studi di Cagliari, Italy) and Maura Rosi (Universita di Pisa, Italy) for advice and insights into their own work on ejecta samples collected at Rabaul. Jon Pallister (Chief, Volcano Disaster Assistance Program USGS Cascades Volcano Observatory, WA, US) for volcanological advice and Catherine Skinner (Department of Geology and Geophysics, Yale University, CT, US) for guidance on the characterisation of fibres. Ken Donaldson and Fiona Murphy at the MRC Centre for Inflammation Research at the University of Edinburgh, for carrying out the Erythrocyte Lysis Analysis. Frank Kelly at the Lung Biology Group at King's College, London for advice regarding the oxidative capacity results. Ben Williamson, Camborne School of Mines, for comments and advice. The authors would finally like to thank Alan Brooker of Renishaw plc. for the use of their Raman-SEM.

684 **References**

685 Africano F, Bernard A (2000) Acid alteration in the fumarolic environment of Usu
686 volcano, Japan. J Volcanol Geotherm Res 97:475-495.

687 Armienta MA, Martin-Del Pozzo AL, Espinasa R, Cruz O, Ceniceros N, Aguayo A,
688 Butron MA (1998) Geochemistry of ash leachates during the 1994–1996 activity of
689 Popocatepetl. App Geochem 13(7):841–850.

690 Ayres JG, Brom P, Cassee FR, Castranova V, Donaldson K, Ghio A, Harrison RM, Hider
691 R, Kelly F, Kooter IM, Marano F, Maynard RL, Mudway I, Nel A, Sioutas C,
692 Smith S, Baeza-Squiban A, Cho A, Duggan S, Froines J (2008) Evaluating the
693 toxicity of airborne particulate matter and nanoparticles by measuring oxidative
694 stress potential – A workshop report and consensus agreement. Inhal Toxicol
695 20:75-99.

696 Bargar KE, Keith TEC, Trusdell FA (1995) Fluid-inclusion evidence for past temperature
697 fluctuations in the Kilauea East Rift Zone geothermal area, Hawaii. Geothermics
698 24(5-6):639-659.

699 Baxter PJ, Bonadonna C, Dupree R, Hards VL, Kohn SC, Murphy MD, Nichols A,
700 Nicholson RA, Norton G, Searl A, Sparks RSJ, Vickers BP (1999) Cristobalite in
701 volcanic ash of the Soufriere Hills volcano, Montserrat, British West Indies.
702 Science 283(5405):1142-1145.

703 Blong R, McKee C (1995) The Rabaul eruption 1994 – Destruction of a town. Natural
704 Hazard Research Centre, Macquarie University, Sydney, 52pp.

705 Burilkov T, Michailova-Dotschewa L (1990) Dangers of exposure to dust extraction and
706 production of natural gypsum. Wiss Umwelt 0(2):89-91. Abstract from EMBASE
707 91094689.
708 Clouter A, Houghton CE, Bowskill CA, Hibbs LR, Brown RC, Hoskins JA (1997) Effect
709 of inhaled fibres on the glutathione concentration and gamma-glutamyl
710 transpeptidase activity in lung type II epithelial cells, macrophages, and
711 bronchoalveolar lavage fluid. Inhal Toxicol 9(4):351-367.
712 Clouter A, Houghton CE, Bowskill CA, Hoskins JA, Brown RC (1996) An in vitro/in
713 vivo study into the short-term effects of exposure to mineral fibres. Exp Toxicol
714 Pathol 48(6):484-486.
715 Cronin SJ, Sharp DS (2002) Environmental impacts on health from continuous volcanic
716 activity at Yasur (Tanna) and Ambrym, Vanuatu. Int J Envir Health Res 12:109–
717 123.
718 Cronin SJ, Hedley MJ, Smith RG, Neall VE (1997) Impact of Ruapehu ash fall on soil
719 and pasture nutrient status 1. October 1995 eruptions. NZ J Agr Res 40:383–395.
720 Cullen RT, Jones AD, Miller BG, Donaldson K, Davis JMG, Wilson M, Tran CL (2002)
721 Toxicity of volcanic ash from Montserrat. Report No. TM/02/01, Institute of
722 Occupational Medicine, Edinburgh, p. 55.
723 Cunningham HS, Turner SP, Patia H, Wysoczanski R, Nichols ARL, Eggins S, Dosseto
724 A (2009) (210Pb/226Ra) variations during the 1994-2001 intracaldera volcanism at
725 Rabaul caldera. J Volc Geotherm Res 184:416-426.
726 Einbrodt HJ (1988) The health risks by dusts of calcium sulfate (Ger.). Wiss Umwelt,
727 0(4):179- 181. Abstract from EMBASE 89261036.

728 Fruchter JS, Robertson DE, Evans JC, Olsen KB, Lepel EA, Laul JC, Abel KH, Sanders
729 RW, Jackson PO, Wogman NS, Perkins RW, Van Tuyl HH, Beauchamp RH,
730 Shade JW, Daniel JL, Erikson RL, Sehmel GA, Lee RN, Robinson AV, Moss OR,
731 Briant JK, Cannon WC (1980) Mount St. Helens ash from the 18 May 1980
732 eruption: chemical, physical, mineralogical, and biological properties. Science
733 209(4461): 1116– 1125.
734 Fubini B, Hubbard A (2003) Reactive Oxygen Species (ROS) and Reactive Nitrogen
735 Species (RNS) generation by silica inflammation and fibrosis. Free Rad Biol Med
736 34(12):1507-1516.
737 Fubini B, Fenoglio I, Elias Z, Poirot O (2001) Variability of biological responses to
738 silicas: effect of origin, crystallinity, and state of surface on generation of reactive
739 oxygen species and morphological transformation of mammalian cells. J Environ
740 Pathol Toxicol Oncol 20(Suppl. 1):95–108.
741 Fubini B, Otero Arean C (1999) Chemical aspects of the toxicity of inhaled mineral
742 dusts. Chem Soc Rev 28:373–381.
743 Fubini B, Mollo L, Giamello E (1995) Free radical generation at the solid/liquid interface
744 in iron containing minerals. Free Radic Res 23(6):593–614.
745 Ghio AJ, Kennedy TP, Whorton AR, Crumbliss AL, Hatch GE, Hoidal JR (1992) Role of
746 surface complexed iron in oxidant generation and lung inflammation induced by
747 silicates. Am J Physiol 263:511-517.
748 Global Volcanism Program (2002-) Global Volcanism, 1968 to the Present. Venzke E,
749 Wunderman RW, McClelland L, Simkin T, Luhr JF, Siebert L, Sennert S,
750 Mayberry G (eds.). Smithsonian Institution, Global Volcanism Program Digital

751 Information Series, GVP-4. http://www.volcano.si.edu/reports/. Accessed 1 Apr
752 2009.
753 Greene HG, Tiffin DL, McKee CO (1986) Structural deformation and sedimentation in
754 an active caldera, Rabaul, Papua New Guinea. J Volc Geotherm Res 30:327-356.
755 Gregg SJ, Sing KSW (1982) Adsorption, surface area and porosity, 2nd edn. Academic
756 Press, London.
757 Handbook of Minerals Raman spectra. Laboratoire de Sciences de la Terre ENS-Lyon
758 France. http://www.ens-lyon.fr/LST/Raman/index.php. Accessed 24 July 2008.
759 Hardy JA, Aust AE (1995) Iron in asbestos chemistry and carcinogenicity. Chem Rev
760 95:97-118.
761 Harrison RM, Yin J (2000) Particulate matter in the atmosphere: which particle properties
762 are important for its effects on health? Sci Total Environ, 249**:**85–101.
763 Heal MR, Ellton RA, Hibbs LR, Agius RM, Beverland IJ (2009) A time-series study of
764 the health effects of water-soluble and total-extractable metal content of airborne
765 particulate matter. Occup Environ Med 66(9):636-638.
766 Heming RF (1974) Geology and petrology of Rabaul caldera, Papua New Guinea. Geol
767 Soc Amer Bull 85:1253-1264.
768 Hinkley TK, Smith KS (1982) Leachate chemistry of ash from the May 18, 1980 eruption
769 of Mount St. Helens, Washington. USGS Professional Paper 1397-B.
770 Hnizdo E, Murray J (1998) Risk of pulmonary tuberculosis relative to silicosis and
771 exposure to silica dust in South African gold miners. Occup Environ Med 55:496-
772 502.

773 Horwell CJ, Le Blond JS, Michnowicz SAK, Cressey G. Cristobalite in a rhyolitic lava
774 dome: Evolution of ash hazard. Bull Volcanol, in press.
775 Horwell CJ, Stannett GW, Andronico D, Bertagnini A, Fenoglio I, Fubini B, Le Blond
776 JS, Williamson BW. A mineralogical health hazard assessment of Mt. Vesuvius
777 volcanic ash. J Volc Geotherm Res, Submitted.
778 Horwell CJ, Michnowicz SAK, Le Blond JS. Report on the mineralogical and
779 geochemical characterisation of Hawai'i ash for the assessment of respiratory
780 health hazard. Report issued to the Hawai'i Volcano Observatory, USGS, 2008.
781 Horwell CJ (2007) Grain size analysis of volcanic ash for the rapid assessment of
782 respiratory health hazard. J Environ Monit 9:1107-1115.
783 Horwell CJ, Fenoglio I, Fubini B (2007) Iron-induced hydroxyl radical generation from
784 basaltic volcanic ash. Earth Planet Sci Lett 261:662-669.
785 Horwell CJ, Baxter PJ (2006) The respiratory health hazards of volcanic ash: a review for
786 volcanic risk mitigation. Bull Volcanol 69:1-24.
787 Horwell CJ, Fenoglio I, Ragnarsdottir KV, Sparks RSJ, Fubini B (2003a) Surface
788 reactivity of volcanic ash from the eruption of Soufrière Hills volcano, Montserrat,
789 with implications for health hazards. Environ Res 93(2):202–215.
790 Horwell CJ, Sparks RSJ, Brewer TS, Llewellin EW, Williamson BJ, (2003b), The
791 characterisation of respirable volcanic ash from the Soufriere Hills Volcano,
792 Montserrat, with implications for health hazard. Bull Volcanol 65:346-362.
793 Hoskins JA (2001) Mineral fibres and health. Indoor Built Environ 10(3-4):244-251.

794 IARC (International Agency for Research on Cancer) (1997) Silica and some silicates,
795 IARC Monographs on the Evaluation of Carcinogenic Risk of Chemicals to
796 Humans, vol 42. Lyon, France, p 289.
797 IARC (1993) Cadmium and cadmium compounds, IARC Monographs on the Evaluation
798 of Carcinogenic Risk of Chemicals to Humans, vol 58. Lyon, France, p 119.
799 IARC (1980) Some metals and metallic compounds, IARC Monographs on the
800 Evaluation of Carcinogenic Risk of Chemicals to Humans, vol 23. Lyon, France, p
801 39.
802 Johnson RW, McKee C, Eggins SM, Woodhead JD, Arculus J, Chappell BW (1995)
803 Taking petrologic pathways toward understanding Rabaul's restless caldera. EOS
804 Transations, American Geophysical Union B76, 171.
805 Kane AB (1996) Mechanisms of Mineral Fibre Carcinogenesis. In: Kane AB, Boffetta P,
806 Saracci R, Wilburn JD (eds) Mechanisms of Fibre Carcinogenesis. Lyon:
807 International Agency for Research on Cancer, 11-34.
808 Kelly FJ (2003) Oxidative stress: its role in air pollution and adverse health effects.
809 Occup Environ Med 60:612-616.
810 Kelly FJ, Mudway I, Blomberg A, Frew AJ, Sanström T (1999) Altered lung antioxidant
811 status in patients with mild asthma. Lancet 354:482-483.
812 Kullman GJ, Jones WG, Cornwell RJ, Parker JE (1994) Characterisation of air
813 contaminants formed by the interaction of lava and sea water. Environ Health
814 Perspect 102(5):478-482.
815 Le Bas MJ, Streckeisen AL (1991) The IUGS systematics of igneous rocks. J Geol Soc
816 Lond 148:825-833.

817 Le Blond JS, Cressey G, Horwell CJ, Williamson B J (2009) A rapid method for
818 quantifying single mineral phases in heterogeneous natural dust using X-ray
819 diffraction. Powd Diffrac. 24(1):17-23.
820 Li N, Hao M, Phalen RF, Hinds W, Nel E (2003) Particulate air pollutants and asthma: a
821 paradigm for the role of oxidative stress in PM-induced adverse health effects. Clin
822 Immunol 3:250-265.
823 McKee CO, Johnson RW, Lowenstein PL, Riley SJ, Blong RJ, Desaintours P, Talai B
824 (1985) Rabaul caldera, Papua New Guinea – Volcanic hazards, surveillance, and
825 eruption contingency planning. J Vol Geotherm Res 23:195-237.
826 MDHS (Method for the Determination of Hazardous Substances) (1998) Health and
827 Safety laboratory. Health and Safety Executive, C10. No. 87: Fibres in Air.
828 Mudway IS, Stenfors N, Duggan ST, Roxborough H, Zeilinski H, MArklund SL,
829 Blomberg A, Frew AJ, Sanström T, Kelly FJ (2004) An in vitro and in vivo
830 investigation of the effects of diesel exhaust on human airway lining fluid
831 antioxidants. Arch Biochem Biophys 423:200-212.
832 Nairn IA, McKee CO, Talai B, Wood CP (1995) Geology and eruptive history of the
833 Rabaul caldera area, Papua New Guinea. J Vol Geotherm Res 69:255-284.
834 Nairn IA, Talai B, Wood C P, McKee C O (1989) Rabaul Caldera, Papua New Guinea -
835 1:25,000 reconnaissance geological map and eruption history. New Zeal Geol Surv
836 Dept Sci Ind Res, geol map.
837 Ohba T, Nakagawa M (2003) Minerals in volcanic ash. 2: non-magmatic minerals. Glob
838 Environ Res 6(2):53-59.

839 Oakes D, Douglas R, Knight K, Wusteman M, McDonald JC (1982) Respiratory effects
840 of prolonged exposure to gypsum dust. Ann Occup Hyg 26:833-840.
841 Reich M, Zúñiga A, Amigo Á, Vargas G, Morata D, Palacios C, Parada MÁ, Garreaud
842 RD (2009) Formation of cristobalite nanofibers during explosive volcanic
843 eruptions. Geol 37(5):435-438.
844 Rice TM, Clarke RW, Godleski JJ, Al Mutairi E, Jiang NF, Hauser R, Paulauskis JD
845 (2001) Differential ability of transition metals to induce pulmonary inflammation.
846 Toxicol Appl Pharmacol 177: 46–53.
847 Risacher F, Alonson H (2001) geochemistry of ash leachates from the 1993 Lascar
848 eruption, northern Chile. Implication for recycling of ancient evaporates. J
849 Volcanol Geotherm Res 109:319-337.
850 Roggensack K, Williams SN, Schaefer SJ, Parnell Jr RA (1996) Volatiles from the 1994
851 eruptions of Rabaul: Understanding large caldera systems. Science 273(5274):490-
852 493.
853 Schepers GWH, Durkan TM, Delahant AB (1955) The biological effects of calcined
854 gypsum dust. AMA Arch Ind Health 12:329-347.
855 Shi X, Mao Y, Daniel LN, Saffiotti U, Dalal NS, Vallyathan V (1995) Generation of
856 reactive oxygen species by quartz particles and its implication for cellular damage.
857 Appl Occup Environ Hyg 10:1138–1144.
858 Skinner HCW, Ross M, Frondel C (1988) Asbestos and other fibrous materials:
859 mineralogy, crystal chemistry, and health effects. Oxford University Press, US.
860 Skoza L, Snyder A, Kikkawa Y (1983) Ascorbic acid in bronchoalveolar wash. Lung
861 161:99-109.

862 Smith DB, Zielinski RA, Rose Jr WI (1982) Leachability of uranium and other elements
863 from freshly erupted volcanic ash. J Volcanol Geotherm Res 13:1–30.
864 Smith K (2001) Environmental Hazards: Assessing Risk and Reducing Disaster, 3rd edn.
865 Routledge, 171-173pp.
866 teWaterNaude JM, Ehrlich RI, Churchyard GJ, Pemba L, Dekker K, Vermeis M, White
867 NW, Thompson ML, Myers JE (2006) Tuberculosis and silica exposure in South
868 African gold miners. Occup Environ Med 63:187-192.
869 US Department of Heath and Human Service (2006) EPA/IRIS United States
870 Environmental Protection Agency/Integrated Risk Information System data base.
871 http://cfpub.epa.gov/ncea/iris/index.cfm. Accessed 25 Mar 2009.
872 Vallyathan V, Robinson V, Reasor M, Stettler L, Bernstein R (1984) Comparative in
873 vitro cytotoxicity of volcanic ashes from Mount St. Helens, El Chichon, and
874 Galunggung. J Toxicol Environ Health 14:641-654.
875 van der Vleit A, O'Neill CA, Cross CE, Koostra JM, Volz WG, Halliwell B, Louie S
876 (1999) Determination of low-molecular-mass antioxidant concentrations in human
877 respiratory tract lining fluids. Am J Physiol 276:L289-L296.
878 Varekamp JC, Luhr JF, Prestegaard KL (1984) The 1982 eruptions of El Chichon
879 Volcano (Chiapas, Mexico): character of the eruptions, ash-fall deposits, and gas
880 phase. J Volcanol Geotherm Res 23:39– 68.
881 World Health Organisation (2006) Air Quality Guidelines Global Update 2005. Geneva:
882 WHO.
883 World Health Organisation (1986) Asbestos and other natural mineral fibres.
884 Environmental Health Criteria 53. Geneva: WHO

885 Willis RJ, Kratzig CC (1974) Ascorbate acid in rat lung. Biochem Biophys Res Commun
886 59(4):1250-1253.
887 Witham CS Oppenheimer C, Horwell CJ (2005) Volcanic ash-leachates: a review and
888 recommendations for sampling methods. J Volc Geotherm Res 114(3-4):299-326.
889 Wood CP, Nairn IA, McKee CO, Talai B (1995) Petrology of the Rabaul caldera area,
890 Papua New Guinea. J Volc Geotherm Res 69:285-302.
891 Yano E, Yokoyama Y, Nishii S (1986) Chronic pulmonary effects of volcanic ash: an
892 epidemiologic study. Arch Environ Health 41(2):94-99.
893

894 **Figure captions**

895 **Figure 1** Map of Rabaul caldera, PNG, showing the locations of the vents within the
896 caldera (based on Greene et al. 1986; Heming, 1974)

897 **Figure 2** Map of PNG showing the location of the volcanoes

898 **Figure 3** Results from XRF analyses of volcanic ash samples, on a TAS (total alkali
899 versus silica content, after Le Bas and Streckeisen 1991) plot

900 **Figure 4** SEM SE image of Tav R2 showing a cross section through a fibre

901 **Figure 5** SEM SE image of Manam ash showing a fibre with small particles adhering to
902 the surface

903 **Figure 6(a)** SEM image of R3 sample in BSE, **b)** X-ray analysis spectrum 1, c) X-ray
904 analysis spectrum 2. The location of both spectra are labelled in 6a

905 **Figure 7(a)** SEM BSE image Tav R2, which shows a typical fibre in the centre, **b)**, **c)**
906 and **d)** are EDX maps of Ca, S and Si (respectively) within the image seen in Fig. 7(a)

907 **Figure 8(a)** SEM BSE image of fibres in Tav R3, **b)** the EDX spectra (location indicated
908 in 8(a)), **c)** Raman spectra for a fibre in Tav R3 (seen in 8(a)) with library spectra for
909 gypsum and anhydrite (Handbook of Minerals Raman Spectra)

910 **Figure 9** Production of hydroxyl radicals (per unit surface area) for the samples over the
911 60 min experiments. Each value is the average of at least two experiments with error bars
912 representing the standard error

913 **Figure 10** Amount of Fe removed as **a)** Fe^{2+} and **b)** total Fe during 9 days of incubation
914 with chelators. The Fe removed is expressed as amount per unit surface area

915 **Figure 11** Amount of hydroxyl radicals generated after 30 min from the start of
916 incubation versus total amount of iron extracted by chelators after 7 days. **a)** PNG

917 samples; **b)** PNG samples and four samples previously used by Horwell et al. 2007b.

918 Mon = Soufrière Hills, Montserrat (5/6/99); Pin = Pinatubo (1991); Cer = Cerro Negro

919 (1995); Etna = Mt. Etna, Sicily (2002)

920 **Figure 12** Ascorbate depletion in the present of 10 μg ml^{-1} of particulate or ash sample

921 **Figure 13** Relationship between the quantity of particles below 4 μm and the wt. % SiO_2

922 in the volcanic ash samples tested

923 Table 1 Sample information and summary of the main analytical techniques in this paper

Sample Name	Volcano	Date erupted	Date collected	Location	Collected by	Analysis							
						Malvern	XRF	SEM-RAMAN	XRD	BET	EPR	Leachate	Haemolysis
Lang L5	Langila	01/04/63	01/04/63	9.5 km from vent	Prof W Rose	√		√	√				
Vul 94N	Vulcan	19/09/94	09/94	2.5 km N of Vulcan	RVO	√	√		√	√	√		
Vul 94S	Vulcan	19/09/94	09/94	1 km S from base of Vulcan	RVO	√	√		√				
Vul 94W	Vulcan	19/09/94	09/94	1 km W from base of Vulcan	RVO	√	√						
Tav 98a	Tavurvur	13/05/98	13/05/98	2 km NW of Tavurvur	RVO	√							
Tav 98b	Tavurvur	12/06/98	12/06/98	RVO	RVO	√							
Tav 98c	Tavurvur	17/07/98	17/07/98	Matupit Island	BGS	√	√		√				
Tav 98d	Tavurvur	19/10/98	19/10/98	Matupit Island	RVO	√	√	√	√	√	√		
Man 98	Manam	01/11/98	01/11/98	4 km SW of Manam summit	RVO	√	√		√	√	√		
Tav 99a	Tavurvur	15/02/99	15/02/99	RVO	RVO	√							
Tav 99b	Tavurvur	25/08/99	25/08/99	RVO	RVO	√							
Tav 00	Tavurvur	01/09/00	01/09/00	Rabaul airport	RVO	√	√	√	√	√	√		
Tav 05	Tavurvur	05-06/10/05	05-06/10/05	RVO	RVO	√	√	√	√	√	√		
Lang 07	Langila	02/06/07	02/06/07	9.5 km NW from vent	RVO	√	√	√	√	√	√		
Tav 07	Tavurvur	03/10/07	03/10/07	RVO	RVO	√							
Tav R2	Tavurvur	09/04/08	09/04/08	3-4 km from vent, collected on frangipani leaves	Dr P Baxter	√	√	√	√	√	√	√	√
Tav R3	Tavurvur	09/04/08	09/04/08	3-4 km from vent, collected on frangipani leaves	Dr P Baxter	√	√	√	√				
Tav R4	Tavurvur	10/04/08	10/04/08	At foot of Tavurvur	Dr P Baxter	√	√		√	√	√		
Tav R6	Tavurvur	12/04/08	12/04/08	At foot of Tavurvur	Dr P Baxter	√	√		√				

924 Table 2 Results in cumulative vol. % the Malvern Mastersizer 2000. Results are an average from three runs. The potential health effects (Horwell et

925 al. 2007) are defined below

	Sample Name																		
Particle size (µm)	**Lang L5**	**Vul 94N**	**Vul 94S**	**Vul 94W**	**Tav 98a**	**Tav 98b**	**Tav 98c**	**Tav 98d**	**Man 98**	**Tav 99a**	**Tav 99b**	**Tav 00**	**Tav 05**	**Lang 07**	**Tav 07**	**Tav R2**	**Tav R3**	**Tav R4**	**Tav R6**
sub- 4	6.2	6.5	4.7	5.6	6.6	5.4	5.2	6.5	3.3	2.1	4.3	4.5	5.2	3.5	5.2	4.7	4.3	4.5	4.2
sub-10	13.6	13.6	10.6	11.8	15.2	12.6	11.6	15.0	7.3	4.3	10.0	11.9	11.6	8.6	12.8	10.7	10.1	10.7	10.1
sub-15	18.8	18.7	14.7	16.1	20.9	17.7	16.8	21.5	10.7	6.3	14.0	18.7	16.5	12.9	18.9	15.6	15.0	14.9	14.3
sub-63	47.8	47.7	36.5	40.8	48.4	41.1	46.8	51.7	34.3	23.5	32.3	50.7	44.0	41.3	49.7	45.6	45.4	33.0	38.3

926

Particle size (µm)	**Health effects***
sub-4	'Respirable' fraction – can enter the alveoli where chronic disease could occur with long-term exposure
sub-10	'Thoracic' fraction – can enter past the bronchus, where bronchitis, asthma and other acute diseases may be triggered in susceptible people
sub-15	Can enter the throat, causing rhinitis, laryngitis and irritation

927 Table 3 Results of the leachate analysis for Tav R2

Element	$Mgkg^{-1}$
Fe	<0.1
As	0.15
Cd	0.023
Co	0.05
Cr	<0.05
Cu	1.5
Mn	10.2
Ni	0.075
Pb	<0.05
Zn	2.85
F	21.8

928

929 Table 4 Results from the IAS method for quantifying the cristobalite phases within the
930 volcanic ash samples (the error is estimated at 1-3 wt. %) and the results of the BET
931 analysis to determine the specific surface area (SSA) of the bulk ash samples

	XRD	SSA	
Sample Name	**wt. % cristobalite**	**m^2g^{-1}**	**Error (+/-m^2g^{-1})**
Vul 94N	2.27	2.7	0.0034
Vul 94S	2.67	-	-
Vul 94W	1.19	-	-
Tav 98c	4.60	-	-
Tav 98d	5.01	0.5	0.0009
Man 98	1.93	0.2	0.0001
Tav 00	1.96	2.0	0.0033
Tav 05	2.40	0.2	0.0006
Lang 07	2.42	0.5	0.0013
Tav R2	2.04	0.6	0.0012
Tav R3	2.37	-	-
Tav R4	2.53	0.3	0.0025
Tav R6	3.06	-	-

932 Table 5 Results of the XRF analysis for the volcanic ash samples (wt. %)

Sample Name	SiO_2	TiO_2	Al_2O_3	Fe_2O_3	MnO	MgO	CaO	Na_2O	K_2O	P_2O_5	SO_3	LOI	Total
Vul 94N	61.21	0.85	15.29	6.29	0.16	1.90	4.64	4.37	2.38	0.32	0.18	2.35	99.83
Vul 94S	61.94	0.89	15.39	6.25	0.16	1.78	4.22	4.42	2.47	0.35	0.02	1.96	99.87
Vul 94W	61.45	0.89	15.46	6.38	0.16	1.89	4.64	4.49	2.38	0.36	0.02	1.60	99.72
Tav 98c	60.34	0.86	15.90	6.84	0.16	2.59	5.88	4.29	2.16	0.32	0.17	0.47	99.99
Tav 98d	60.59	0.90	15.58	6.61	0.16	2.48	5.14	4.48	2.37	0.34	0.09	0.64	99.37
Man 98	51.25	0.35	15.93	9.90	0.16	7.75	11.42	2.50	0.68	0.12	0.05	0.64	99.29
Tav 00	54.28	0.81	14.61	6.73	0.13	2.48	6.31	3.22	1.67	0.24	2.62	-0.02	99.45
Tav 05	62.28	0.90	15.81	6.43	0.16	1.90	4.72	4.67	2.50	0.33	0.01	6.34	99.87
Lang 07	55.89	0.55	17.00	9.36	0.18	3.46	8.00	2.96	1.76	0.21	0.14	0.17	99.81
Tav R2	61.76	0.88	15.78	6.40	0.16	1.89	4.83	4.66	2.49	0.35	0.08	0.29	99.72
Tav R3	61.77	0.89	15.79	6.50	0.16	1.94	4.86	4.62	2.46	0.34	0.08	0.44	99.74
Tav R4	61.26	0.90	15.74	6.81	0.17	2.11	5.18	4.56	2.38	0.36	0.01	0.32	99.64
Tav R6	61.44	0.90	15.77	6.68	0.16	2.12	5.03	4.59	2.40	0.35	0.08	0.17	99.87

933 Table 6 Averaged results (% haemolysis) for Tav R2

Sample Name	Mean % haemolysis*	SSA $m^2 g^{-1}$	Haemolysis (% Haemolysis per unit surface area)
Negative Control	0.00	-	0.00
Rutile	1.07	27.5	0.04
Anatase	3.05	258	0.01
DQ12 quartz	32.29	10.1	3.20
Tav R2	0.71	0.59	1.20
Triton X	100.00	-	100.00

934 *average from three runs

935 Figure 1

936

937 Figure 2

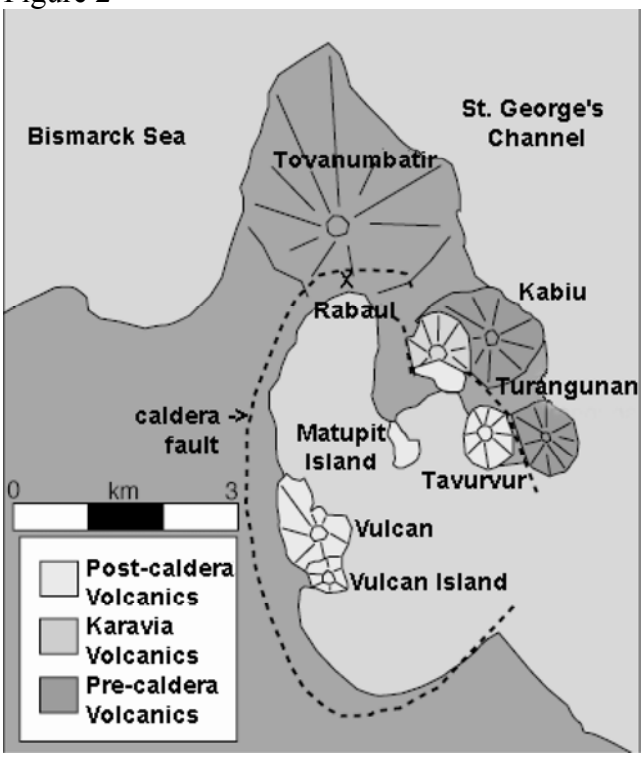

938

939 Figure 3

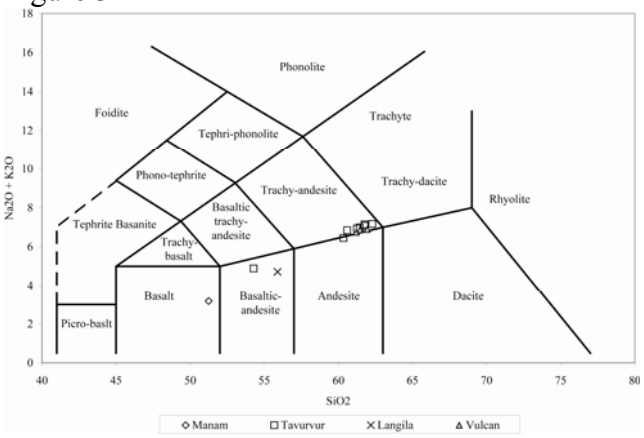

940

941 Figure 4

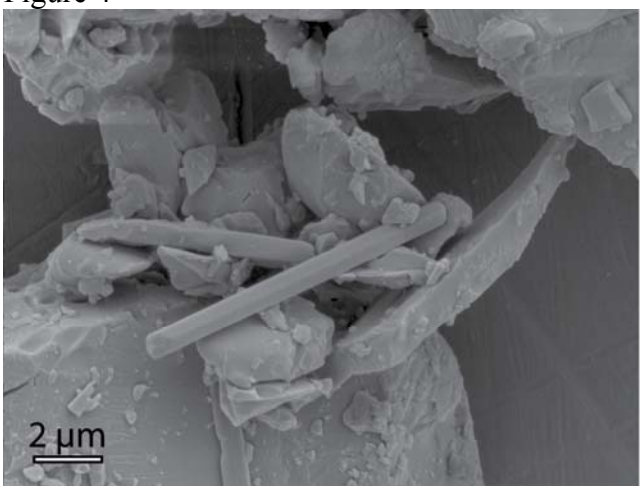

942

943 Figure 5

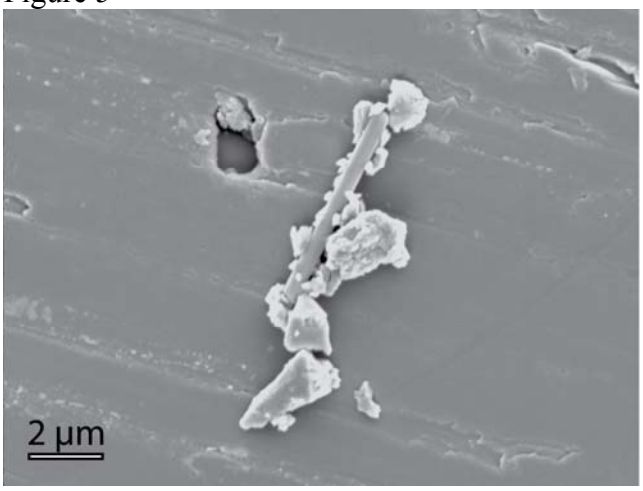

944

945 Figure 6

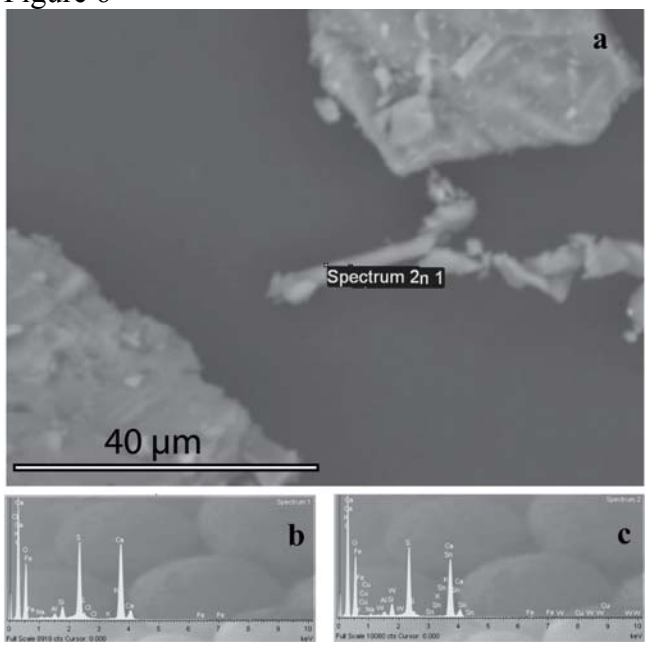

946

947 Figure 7

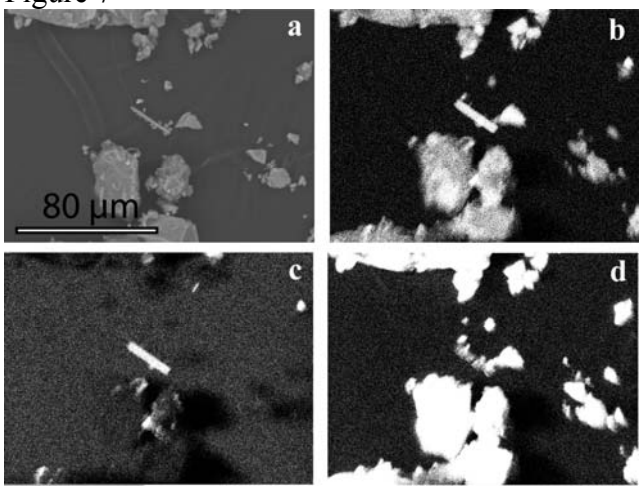

948

949 Figure 8

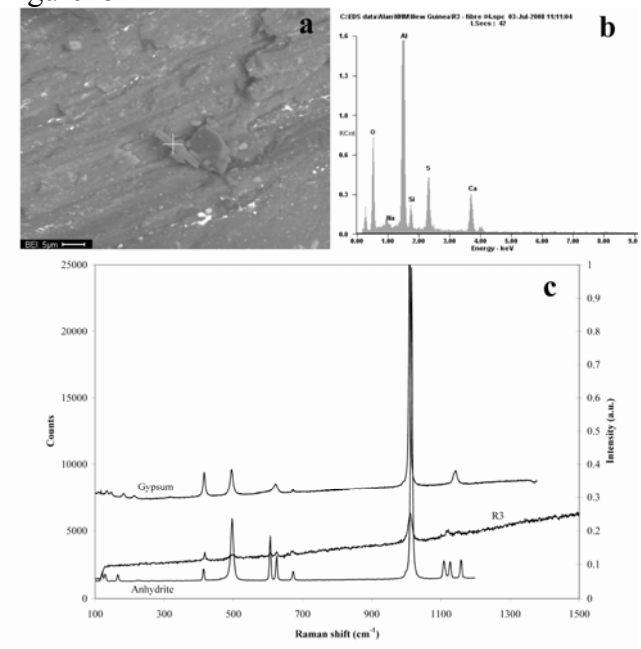

950

951 Figure 9

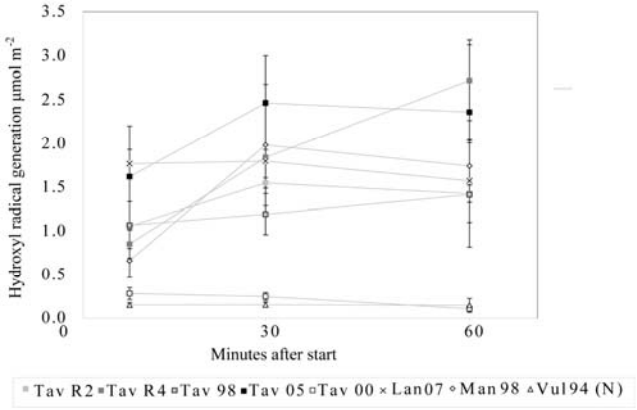

952

953 Figure 10

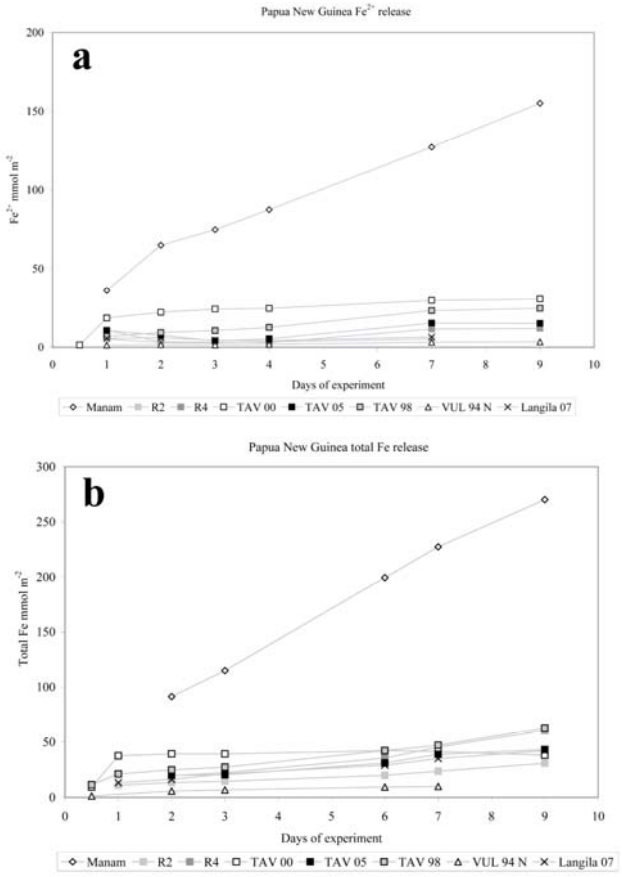

954

955 Figure 11

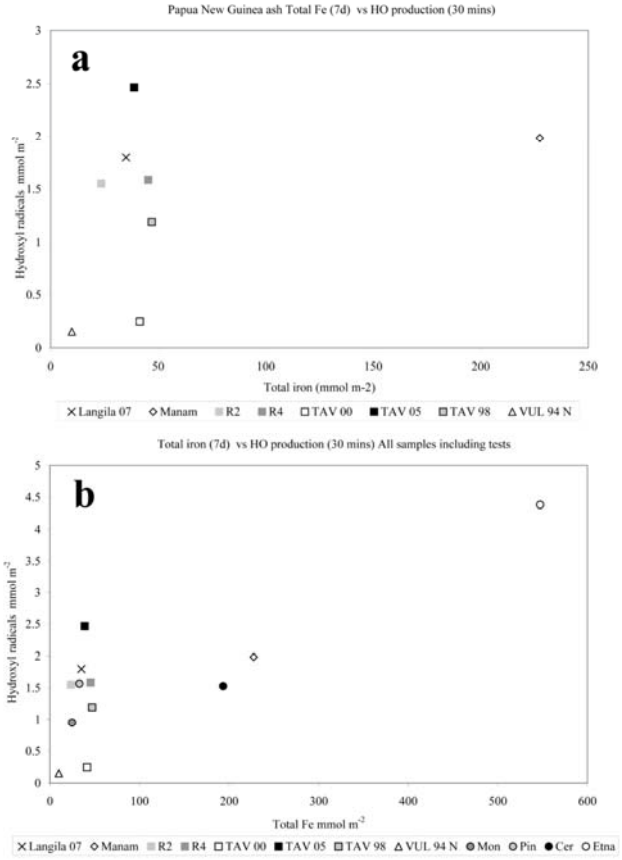

956

957 Figure 12

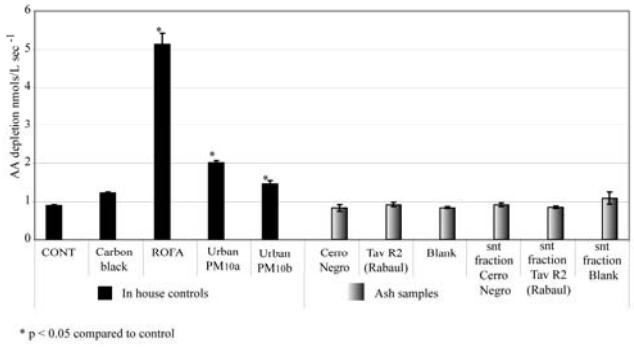

* p < 0.05 compared to control

958

959 Figure 13

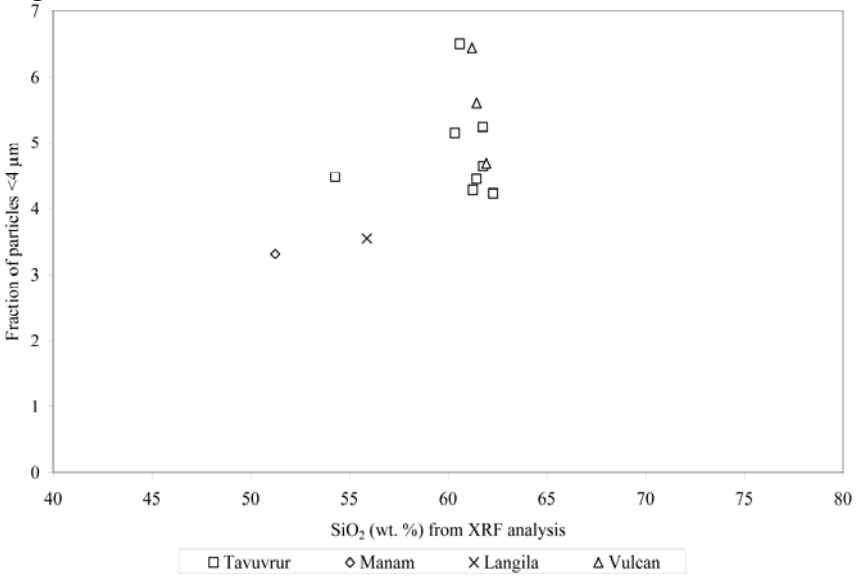

960
961